

Original article

## Homology-based molecular modelling of PLP-dependent histidine decarboxylase from *Morganella morganii*

Fatemeh Sadat Tahanejad<sup>a</sup>, Hossein Naderi-Manesh<sup>b\*</sup>, Bahram Habibinejad<sup>c</sup>,  
Massoud Mahmoudian<sup>d</sup>

<sup>a</sup>Dept. Pharm., Baghiyatollah Univ. Med. Sci., P.O. Box: 19585-698, Tehran, Iran

<sup>b</sup>School of Sciences, Tarbiat Modarres University, Tehran, Iran

<sup>c</sup>Dept. Pharm. Chem., Tabriz Univ. Med. Sci., Tehran, Iran

<sup>d</sup>Dept. Pharm., Iran Univ. Med. Sci., Tehran, Iran

Received 13 July 1999; revised 15 November 1999; accepted 22 December 1999

**Abstract** – The 3-D structural information is a prerequisite for a rational ligand design. In the absence of experimental data, model building on the basis of a known 3-D structure of a homologous protein is at present the only reliable method to obtain structural information. A homology model building study of the pyridoxal 5'-phosphate (PLP)-dependent histidine decarboxylase from *Morganella morganii* (HDC-MM) has been carried out based on the crystal structure of the aspartate aminotransferase from *Escherichia coli* (AAT-EC). The primary sequences of AAT-EC and HDC-MM were aligned by automated alignment procedure. A 3-D model of HDC-MM was constructed by copying the coordinates of the residues from the crystal structure of AAT-EC into the corresponding residues in HDC-MM. After energy-minimization of the resulting 3-D model of HDC-MM, possible active site residues were identified by fitting the substrate (l-histidine) into the proposed active-site. In our model, several residues, which have an important role in the AAT-EC active-site, are located in positions spatially identical to those in AAT-EC structure. The back-bone of the modelled active site pocket is constructed by residues; Gly-92, Gly-93, Thr-93, Ser-115, Asp-200, Ala-202, Ser-229 and Lys-232 together with residues Asn-8, His-119, Thr-171, His-198, Leu-203, His-231, Ser-236 and Ile-238. In the ligand binding site, it appears that the HDC-MM model will position l-histidine (substrate) in the area consisting of the residues; Glu-29, Ser-30, Leu-38, His-231 and Lys-232. The nitrogen atom of the imidazole ring (N2) of the substrate is predicted to interact with the carboxylate group of Ser-30. The  $\alpha$ -carboxylate of histidine points toward the Lys-232 to have electrostatic interaction with its side chain nitrogen atom (N<sub>2</sub>). In conclusion, this combination of sequence and 3-D structural homology between AAT-EC and HDC-MM model could provide insight in assigning the probable active site residues. © 2000 Éditions scientifiques et médicales Elsevier SAS

histidine decarboxylase / pyridoxal-5'-phosphate (PLP) / sequence alignment / molecular modelling / homology modelling

### 1. Introduction

Histidine decarboxylase (HDC, l-histidine decarboxylase, EC 4.1.1.22) [1] catalyses the decarboxylation of l-histidine to histamine [2–4] which is known to be involved in allergic reactions [5], inflammation (via H<sub>1</sub> receptors) and gastric secretion [6, 7] (via H<sub>2</sub> receptors). The recent elucidation of the histaminergic neurone system and the identification of a specific synaptic subtype of the histamine receptors (H<sub>3</sub>) in the brain provides support for its role in neuroregulation [8–10]. Occasional indications can be found in the literature of high histamine levels in some tumours [11–13].

Currently used agents to prevent histamine effects are histamine receptor antagonists, and sometimes drugs, which prevent histamine release from histamine-storing cells (mast cells). Histidine decarboxylase inhibitors may have a promising potential for developing effective and safe agents in the prevention of histamine overproduction conditions [12–14]. They also may have reduced undesired effects and toxicities of the currently used drugs in the therapy of ulcer and allergy.

Despite the manifold physiological effects of histamine, mammalian histidine decarboxylase is still not a fully characterized enzyme, primarily because of its instability and very low concentration in even the richest sources [15–17]. However, extensive characterization of

\* Correspondence and reprints: Naderman@modares.ac.ir

```

Query:   130 LRIKSQVVESQPNGEIDYDDLMMKKIADDKEAHPIIFANIGTTVRGAIDDI AEIQRLKAA 189
          L ++          N +D+D L++ + + + ++ ++F          G ID  E  + L
Sbjct:   142 LEVREYAYYDAENHTLDFDALINSLNEAQAGDVVLFHGCCCHNPTG-IDPTLEQWQTLAQL 200

Query:   190 GIKREDYYLHA-DAALSGMILPFVDDAQPF-TFADGIDSIGVSGH--*KMIG---SPI-PC 241
          ++ +      L  D A G  + +DA+ + +FA      + V++  K +G      + +C
Sbjct:   201 SVEKG--WLPLDFAYQGFARGLEEDAEGRLAFAAMHKELIVASSYSKNFGLYNERVGAC 258

Query:   242 GIVVAKKENVDRI-----SVEIDYIS--AHDKTITGSRNGHTPLM-LWEAIRSHSTEEW 292
          +V A  E VDR      ++ +Y +  AH+ ++ ++ ++ ++ +L  +WE      +  +
Sbjct:   259 TLVAADSETVDRAFSQMKAIRANYSNPPAHGASVVATILSNDALRAIWE----QELTDM 314

Query:   293 KRRITRSLDMAQYAVDRMCKAGIN 316
          ++RI R   M Q  V+ +Q  G N
Sbjct:   315 RQRIQR---MRQLFVNTLQKEGAN 335

```

**Figure 1.** BLASTP2 results obtained from sequence comparison between target protein (HDC-MM) and template (AAT-EC). 'Query' and 'Sbjct' refer to HDC-MM and AAT-EC sequences, respectively. \*The lysine residue (Lys-232), responsible for making internal aldimine with coenzyme (PLP) has been marked by an asterisk.

HDC was carried out on enzyme from *Morganella morganii* (HDC-MM) [18–20], which resembled the mammalian one in requiring pyridoxal 5'-phosphate (PLP) as coenzyme.

So far all HDCs that have been isolated from Gram-negative bacteria [21, 22] or mammals [23–26] use PLP as a coenzyme and have identical subunits, while those from Gram-positive bacteria have a pyruvoyl prosthetic group and have dissimilar large and small subunits [27–31]. The PLP- and pyruvoyl-dependent HDCs represent a rare example of independent evolution leading to very different proteins that catalyse an identical reaction.

Pyridoxal 5'-phosphate is a coenzyme for a number of enzymes which catalyse reactions at C $\alpha$  of amino acid substrates [32] including transamination [33], decarboxylation [34–40], racemization [41] and elimination [42, 43].

Transaminases are the best understood PLP-dependent enzymes and the most significant contribution in the area came from X-ray crystal work on aspartate aminotransferase (AAT) [44–47], which was used as a template to construct the HDC-MM 3-D structure.

HDC from *Morganella morganii* is a tetramer of identical subunits of known amino acid sequence and binds 4 PLP/tetramer. In the HDC-MM structure, as for other PLP-dependent enzymes, PLP is present as an internal aldimine formed with the  $\alpha$ -amino group of the Lys (K-232) residue, which is replaced by l-histidine (substrate) to form an external aldimine [48, 49]. X-ray crystallography and NMR spectroscopy are the only ways to obtain detailed structural information. Unfortunately, these techniques involve elaborate technical procedures and demand proper crystal and/or large quantities of protein.

Comparisons of the tertiary structures of homologous proteins have shown that 3-D structures have been better conserved in evolution than protein primary structures, indicating the feasibility of model building by homology.

The purpose of present work is to apply homology-based molecular modelling techniques to generate a reasonable three-dimensional (3-D) structure for PLP-dependent histidine decarboxylase from *Morganella morganii*.

## 2. Experimental procedures

Several stages were distinguished during the course of the homology model building study.

### 2.1. Sequence alignment

A BLASTP2 data base search (Bork Group's Advanced BLAST2 search service at EMBL, available via the internet at URL <http://www.EMBL-Heidelberg.de>) was applied on the HDC-MM sequence against the Brookhaven Data Bank. We used these results to find the best template to construct a 3-D model of HDC-MM.

The results of the BLASTP2 analysis would support the hypothesis of structural homology between HDC-MM and AAT, sharing the same cofactor and being able to match the PLP-binding lysine and some other residues around the active site (figure 1).

The coordinates of the crystal structure of AAT from *Escherichia coli* (AAT-EC) with 1.8 Å resolution have been taken from the PDB (PDB Entry 1ARS [45]) and protein sequences herein were obtained from the Swiss-Prot. The sequence alignment analysis between the primary amino acid sequences of AAT-EC and HDC-MM

was established using an automated multiple sequence alignment procedure (ClustalW) [50].

Secondary structure predictions were calculated using the PHD method [51]. The PHD program uses evolutionary information as an input to a neural network system to predict secondary structure.

Multiple alignments were adjusted manually by aligning the secondary structure elements of AAT-EC with the corresponding regions in HDC-MM to maximize agreement of primary sequences and the predicted secondary structure.

## 2.2. Homology model building

Molecular modelling was performed on a Silicon graphic Iris Indy workstation using the commercial software package Insight II [52]. X-ray structure coordinates of AAT-EC [45] served as a template to construct the HDC-MM model by amino acid replacements of the matched sequence positions and by making sequence insertions and deletions as required. The conserved regions of the AAT-EC and HDC-MM models were aligned and the coordinates of the overlapping residues were copied from the known AAT-EC structure onto the unknown HDC-MM structure, using the Homology module within Insight II. During this computer mutagenesis, the coordinates of each side chain were maintained as close as possible to the atomic positions of the template structure. The coordinates for sequence insertions and deletions were generated using Homology's FIND LOOP algorithm followed by preliminary model refinement.

For coenzyme docking, the PLP was placed into the HDC-MM model to occupy a position as in the AAT-EC structure. Then, a search was made for close contacts between non-hydrogen atoms and bumps were removed. The handling and visualization of the 3-D molecular structure and the construction of missing H-atoms (at PH = 7.4) were accomplished.

The potential were assigned by using the automatic assignment module of the Insight II package. Charges for enzyme were added by using the automatic charge assignment procedure of this package, but charges for ligands were imported from the MOPAC parameters [53, 54] using PM3 Hamiltonian [55].

For computational methods such as molecular dynamics (MD), molecular mechanics (MM) or a systematic search, an appropriate force field is required which can adequately describe the potential energy surface for enzyme and substrate. In this study we used CFF91 [56] as a force field.

## 2.3. Energy minimization

The energy minimization was carried out with the program Discover. The structure of the HDC-MM was constructed and refined by automated rotamer optimization followed by energy minimization. Conjugate gradient minimization was used until the rms energy gradient was below 0.01 kcal/mol.Å.

For MD simulation, we fixed the backbone of the enzyme and some water molecules in the active site, and the simulations were restricted to the side chains and surface waters. The MD simulation protocol included an initial step of minimization by using the conjugate gradient algorithm, an equilibration time of 5 000 ps and a production time of 100 000 ps. From the conformations of the production time the ten lowest energies were automatically selected and energy minimization of the complete ensemble was performed using the conjugated gradient method.

WHATIF (Module CHECK) [57] and PROCHECK Ver. 3. 4. 2 [58] softwares were used for testing the 3-D structures.

## 2.4. Molecular docking

The l-histidine, in s configuration as substrate, was docked in the energy-minimized 3-D model of HDC-MM. We also docked 2-amino-2-methyl 3(2-benzimidazole) propionic acid (BMP) in the HDC-MM active site as a test compound to predict its inhibitory activity.

The molecular structure of ligands were constructed applying the Insight II package and the initial geometrical parameters, bond lengths and angles for the molecules were taken from the standard geometries implemented in this program. A systematic search and MD simulation were performed in order to obtain the best conformation of the ligands.

Data about probable active sites and important residues involved in the enzyme-substrate interactions were obtained from mutagenesis experiments [19, 65]. According to these data, the ligands were manually docked into their binding cavity using graphical manipulation coupled to continuous energy, distances and hydrogen bond formation monitoring. When a final position was reached, consistent with suitable distances and known pharmacological data, the complex of enzyme-ligand was subjected to minimization. The docking procedure was repeated several times with different initial orientations of the side chains and of the ligands in order to obtain the best possible interaction of the complexes. All calculations were performed on an SGI computer (Silicon Graphics Incorporation).

We studied the HDC-MM in a complete model (including enzyme, coenzyme, substrate or inhibitors) and after minimization, distances, angles, probable H-bonds, interaction energies and the potential energy were measured.

### 3. Results and discussion

We used the BLASTP2 server to detect homology between the sequence of histidine decarboxylase from *Morganella morganii* (HDC-MM) and other proteins with known structure in order to find which structure inside PDB is the best to use as a template. It was found that there is sequence similarity among the sequence of interest and some of the proteins in PDB. All of the matched proteins are functionally distinct from HDC-MM except aspartate aminotransferase from *E. coli* (AAT-EC). This protein belongs to the PLP-dependent system and uses the same cofactor as the target protein.

This profile attributed the highest scores in the range of 111–154 to the known proteins, renin (PDB code 1BIL), penicillin amidohydrolase (PDB code 1PNK), catalase (PDB code 7CAT), tyrosine phenol-lyase (PDB code 1TPL) and triose phosphate isomerase (PDB code 1YPI). Aspartate aminotransferase, which appears to be more distantly related to histidine decarboxylase, occurs at score 109. The decarboxylases and aminotransferases act upon the same substrates, i.e. diverse amino acids.

The AATs are one of the best structurally and functionally characterized groups of PLP-dependent enzymes. An evolutionary relationship between group II amino acid decarboxylases (containing HDCs) and aminotransferases, which belong to the family of B6 enzymes [43], was further indicated by a search with a profile constructed from the aligned sequences of representative enzymes of the family [59]. It is therefore quite natural to consider AAT structures as a reference to which one can try to match HDC sequences.

According to the BLASTP2 analysis (*figure 1*), the percentage of identity and similarity between HDC-MM and AAT-EC sequences are 23 and 48, respectively, accounting for a total of 179 residues overlapping. These results also indicate that the region encompassing the putative PLP binding site is highly conserved.

The sequences of HDC-MM and AAT-EC were aligned using ClustalW multiple sequence alignment software (ver.1.6, March 1996). The alignment was calculated with gap penalties of 8.0, 10.0 and 0.05 for gap elongation penalty. Only minor differences were seen between the two alternatives and the alignment at 10, bearing the least number of gaps was used. This produced an alignment matching 235 residues with 66 identities (*figure 2*).

High sequence homologies seem to be needed in order to obtain models of sufficient quality and because of the low sequence identity between AAT-EC and HDC-MM, the construction of a complete 3-D model of the HDC-MM from the crystal structure of AAT-EC is probably unrealistic. However, comparisons of the tertiary structures of homologous proteins have shown that 3-D structures have been better conserved in evolution than protein primary structures [60].

Even though sequence identity is very low, some indications would justify the assumption of the AAT reaction framework features as being shared by HDC-MM and being able to match the PLP-binding Lys and some of the residues having an important role in the enzyme active site [45]. Further improvement in alignment can be reached using other structural information.

Secondary structure predictions were calculated for HDC-MM and compared with those assigned to AAT-EC. We used the PHD method that is the best secondary structure prediction program [51]. PHD results were used in the alignment. A general agreement in the C-terminal and central part of the alignment (from positions: 146–167, 179–197, 280–315, 350–372 (*figure 2*)) was seen, with 55% of the aligned residues predicted to share the same conformation.

In the absence of experimental data (e.g., X-ray or NMR), homology-based molecular modelling is the only way to build three-dimensional structures of macromolecules. The goal of this study was to provide an active site model with correct sequence assignments and generally correct spatial assignments for the main chain and side chains of residues important to the catalytic mechanisms and substrate specificity of the enzyme.

PLP-dependent decarboxylases play significant roles in a large number of physiologically vital reactions that include the synthesis of several neurotransmitters (histamine and aminobutyric acid from L-histidine & glutamic acid decarboxylases, respectively) and the synthesis of polyamines (putrescine from ornithine and arginine decarboxylases).

A clearer understanding of the active sites would be useful for effectively designing drugs targeting these enzymes.

AAT is composed of two identical subunits which consist of two domains, a large domain and a small one. The coenzyme is bound to the larger domain in a pocket near the subunit interface. The large domain consists of a sharply twisted  $\beta$ -sheet (six parallel and one antiparallel strand) sandwiched by eight  $\alpha$ -helices from both sides. The small domain consists of two  $\beta$ -sheets and five  $\alpha$ -helices [45].

	EEE	HHHHHHHHHHHHHH	EEEE	HHHHHHHHHHHHHH	HHHHHHHHHHHHHH
HDC-MM 1	TL	SINDQNKLDAFWAYCVKNQY FNI G-YP E SAD F DY TNLERFLRF SI NNCGDWGEYCNYL	//	61	LNSFDFEKEVMEYFADL
AAT-EC 1	MFENITAAPAD P I LG LADLF RA DERPGKIN LG I G V YKDETGKTPVLTSVKKAE QYL LENE -	//	76	I PEFGRCTQE LLFGKGS	
	HHHHHH	EEE	HHHHHHHHHHHHHH	HHHHHHHHHHHH	
	EEEE	EEEEEE	H	HHHHHHHHHHHH	EEEE
HDC-MM	FKIPF EQSWG YVTN	GGTEGNMFGCY LGRE I FPDGTL Y YSKDTH	//	121	YSVAKIVKLLRI KSQVVESQ PNGE IDYDDLMMKKI A
AAT-EC	ALINDKRAR TAQTP	GGTGALR VAADF LAKNTSVKRVVWSNPSW	//	144	KSVFNSA-GLEVREY AYYDAENHTLDFDAL I NSLN
	HH	EEEEEEEE	HHHHHHHHHHHHHHHH	EEEEEE	HHHH
				EEEE	HHHHHHHH
	EEEE	HHHHHHHHHHHHHHHH	EEEEHHHHHH	HHH	EEEE
HDC-MM	DDK EAH P I IFAN I G -T TVRGAIDDAE I QKRLKAAG I KR E DYY LHADAALSGMI LPFVDDAQ	//	217	PFT FADG IDS IGVS	
AAT-EC	E AQAG DVVLF - HGCCHNPTG - IDPTLEQWQTLAQL SVE KG -WL P LFD	FAYQGFARGLEEDAE	//	242	AFAAMHKEL IVASS
	EEEE	EE	HHHHHHHHHHHHHH	EEEEEE	HH
				HHHH	EEEE
	EE	EEEEEEEE	EEEEEEEEEE	E	HHHH
HDC-MM	GHKMIGS P I P	//	240	CG IVV AKKENVDR ISVE I DY I SAHDKT ITGSRNGHTP LM	//
AAT-EC	YSKN FGLYNE	//	270	C TLVAADS ETVDRAFSQMKAAL RANYS - NPPAHGASVVA	//
	HHH	EEEE	HHH	HHHHHHHHHHHHHH	HHHHHHHH
				HHHHHHHHHHHHHHHHHHHH	
	HHHHHHHHHHHHHHHHHH	HH	HHH	EEEE	HHHHHHHH
HDC-MM	RSLDMAQYAVDRMQKAGI N	//	317	AWRNK - N S - I TVVFPDPS ERVWREHCLATSGDVAHL I T TAHH LDTVQ I DKL I DD	
AAT-EC	R IQRMQRQ LFNVT L QEKGAN	//	351	S F I I KQ NGMFSF -S GLTKEQV LRLREE FGVYAVASGRVNVAGMT PDNMAP LCE A	
	HHHHHHHHHHHHHHHHHHHH			HH	HHHEEE
				HHHHHHHHHHHHHHHH	EEE
				EEEE	EEEE
				H	HHHHHHHH
	HHHHHHHH				
HDC-MM	VIADFNLHAA				
AAT-EC	IVAVL				
	HHHH				

**Figure 2.** Sequence alignment between target protein (HDC-MM) and template (AAT-EC), ClustalW [50] results. The secondary structural elements have been shown. Regions with deletions are indicated as '/'. *H* and *B* refer to  $\alpha$ -helix and  $\beta$ -sheet secondary structures, respectively.

HDC-MM has a tetrameric structure comprising four identical subunits, each consists of 377 amino acid residues and one PLP forming an internal aldimine bond with a catalytic residue, Lys-232 [48]. A complete 3-D structure of the HDC-MM was determined including all insertions and deletions.

Figure 3 depicts a ribbon presentation of the HDC-MM model, containing coenzyme (PLP) which is bound to a lysine residue, (shown as ball & sticks and sticks, are PLP and Lys-232, respectively).

Experimentally, several residues have been shown to exist at the active site of AAT-EC [45], these conserved residues are: Gly-107, Gly-108, Thr-109, Asp-222, Ala-224, Ser-255 and Lys-258. The corresponding residues for HDC-MM are given in table 1. In the HDC-MM model, these residues are located in positions spatially identical to those in the AAT-EC structure. Additionally, several non-active site residues are highly conserved whose correct placement in the HDC-MM model structure (with respect to those of AAT-EC) supports the

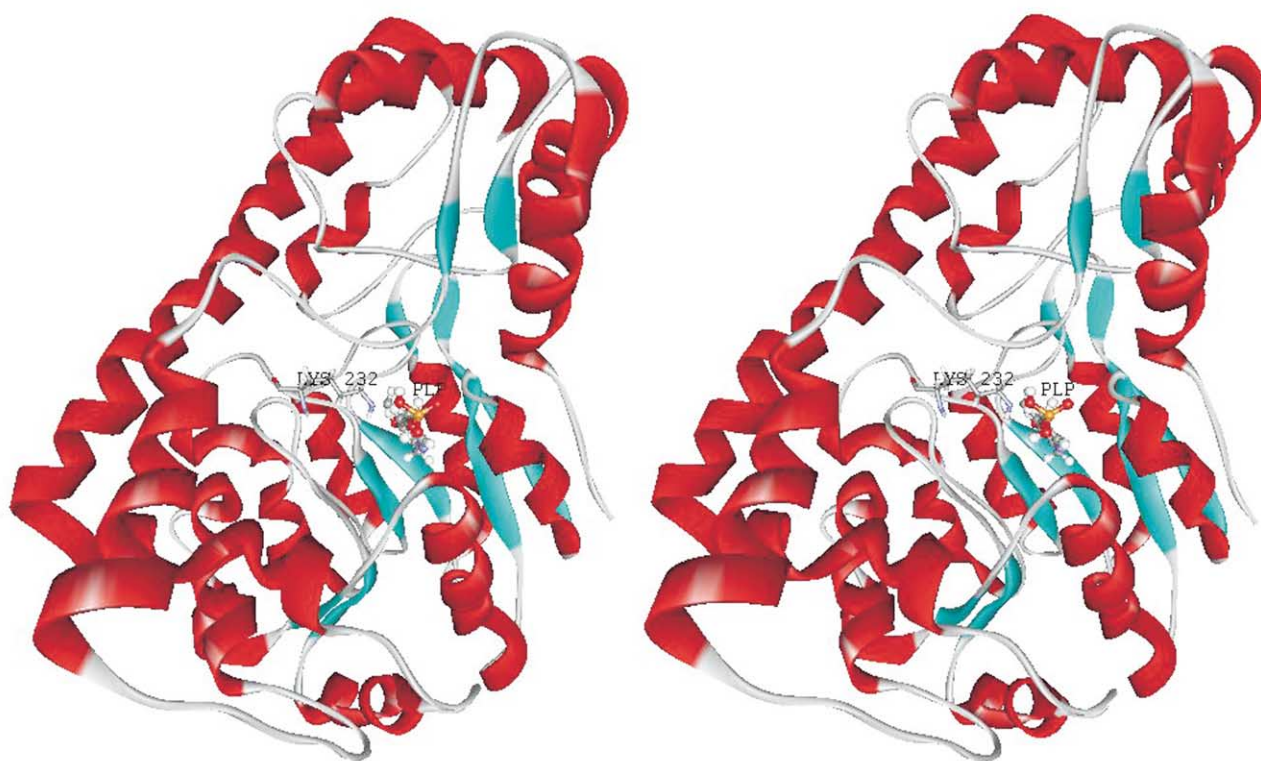


**Figure 3.** Ribbon depiction of the HDC-MM model (target protein). PLP (coenzyme) and lysine residue (Lys-232) which forms schiff base linkage with coenzyme have been shown.  $\alpha$ -Helices appear as solid red coils, while  $\beta$ -strands in green. Ball & sticks and sticks represent PLP and Lys-232, respectively. Colour code: red, oxygen atoms; blue, nitrogen atoms; grey, carbon atoms; white, hydrogen atoms and dark yellow, phosphorous atoms.

general accuracy of our model. All deletions and insertions in the HDC-MM, in reference to the AAT-EC structure, occur in loop regions or at the ends of secondary structural elements (figure 2).

The active site tetrapeptide for decarboxylases was well conserved and contained the finger print sequence

–Ser–X–His–Lys– [19]. This conservation suggests a defined role for the serine and histidine residues for optimal activity. It appears that for HDC-MM, the Ser-229 residue might form a hydrogen bond to the 5'-phosphate ester group of the coenzyme, as in AAT-EC [45].

Some of the active site residues that interact directly with PLP and are proposed to be important to the catalytic mechanism of AAT-EC are structurally conserved in the HDC-MM active site. Lys-232 forms a Schiff base linkage with the carbonyl group of PLP. It has been proposed that His-231 might have different roles such as: acting as a base in deprotonation of substrate during transaldimination and protonation of the quinoid intermediate at C $^{\alpha}$  [42, 61], or forming a hydrogen bond with the phosphate moiety of PLP [38].

According to the mutagenesis data [19], the mutant enzyme K232A lacks activity, suggesting that this lysine residue plays an essential role in catalysis of the decar

**Table I.** Correspondence between the HDC-MM and AAT-EC residues, discussed in the text.

Conserved		Non-conserved	
HDC-MM	AAT-EC	HDC-MM	AAT-EC
Gly-91	Gly-107	Asn-8	Pro-9
Gly-92	Gly-108	His-119	Trp-140
Thr-93	Thr-109	Thr-171	Asn-194
Ser-115	Ser-136	Leu-203	Tyr-225
Asp-200	Asp-222	His-231	Ser-257
Ala-202	Ala-224	His-198	Leu-222
Ser-229	Ser-255	Ser-236	Leu-266
Lys-232	Lys-258	Ile-238	Asn-268

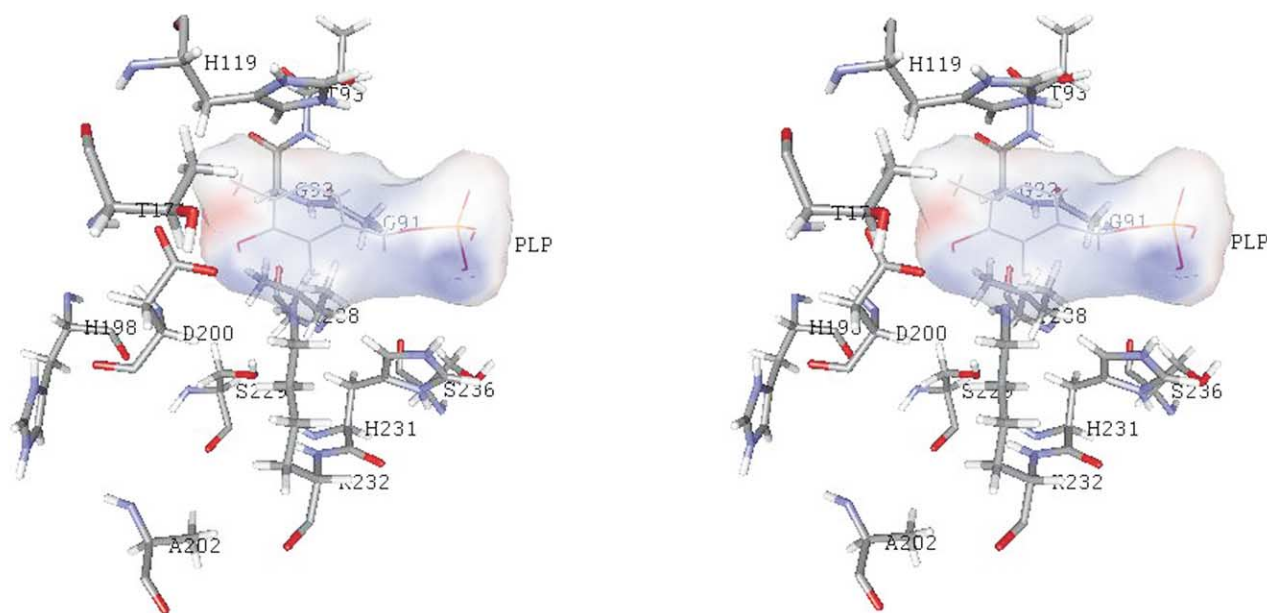


**Figure 4.** Topology of the active site of the HDC-MM model (target protein), displayed in stereoview. Some residues have been omitted to aid visual clarity. The protein residues have been shown as sticks. PLP (coenzyme) is presented as solvent accessible surface.

boxylation process. Mutant proteins, H231Q and H231N were partially active, proposing that His-231 might play some role in hydrogen bonding with coenzyme. The active site residues around the PLP in HDC-MM model have been shown in *figure 4*.

The phosphate group of the PLP interacts with a cluster of hydroxyl from serine and threonine residues (e.g. Ser-115 and Thr-93), as well as main-chain amide nitrogens. The AAT-EC sequence <sup>107</sup>GGT<sup>109</sup> is completely conserved in the HDC-MM sequence according to the sequence alignment, which could function as a proton donor or for stabilization of the PLP phosphate. The main-chain NH's of Gly-108 and Thr-109 (equivalent to Gly-92 and Thr-93 in HDC-MM model, respectively) hydrogen bond with oxygen atom of the phosphate group of PLP (coenzyme). In the HDC-MM active site, coenzyme sits in a pocket surrounded by residues; Gly-91, Gly-92, Thr-93, His-119 and Asp-200. The oxygen atom of Gly-92 is hydrogen bonded to H-O3' of PLP. The imidazole ring of His-119 lies parallel to the pyridine ring of the cofactor (*figure 4*). The HDC-MM sequence <sup>199</sup>ADAAL<sup>203</sup> is partly conserved between two sequences (*figure 2*). The conserved residue, Asp-200, forms an ion pair with the N1 of the pyridinium ring of cofactor PLP. According to the previous results [62], this residue is

necessary to stabilize the positive charge on the protonated N1 of the pyridinium ring.

Ala-202, which is another conserved residue in the mentioned sequence, lies directly behind the ring of cofactor and its methyl side chain could interact with the pyridine ring of PLP. Sequence alignment algorithm associates the serine residue (Ser-115) in the HDC-MM sequence <sup>114</sup>YSKDTH<sup>119</sup> (*figure 2*), which is conserved, in comparison with Ser-136, in AAT-EC sequence <sup>135</sup>VS-NPSW<sup>140</sup>. According to our HDC-MM model, Ser-115 is close to the pyridine ring of PLP and has been conserved among all HDCs.

The large non-polar residue, Trp-140, in AAT-EC makes contact with the pyridine ring of PLP and the  $\alpha$ -carboxylate group of substrate [63]. In the HDC-MM model, His-119 takes this position which is conserved among decarboxylases, indicating its probable significant role in catalysis [38, 64].

X-ray crystal structure of AAT-EC reveals that the O<sub>3'</sub> $\alpha$  atom on the pyridine ring of PLP directly forms a hydrogen bond with the side chains of Tyr-225 and Asn-194. In the HDC-MM model, Leu-203 and Thr-171 are equivalent residues, despite the Leu-203, which is a non-polar residue, Thr-171 might have the same role as Asn-194 in AAT-EC structure.



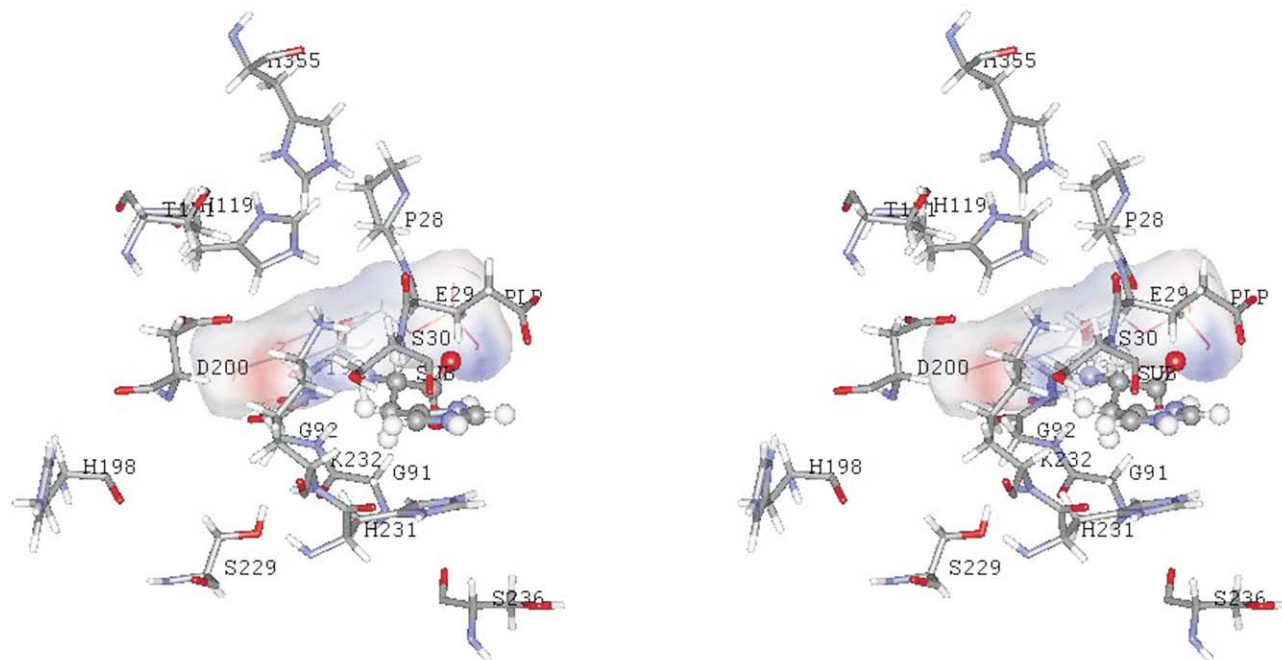


**Figure 5.** Ligand binding site of the HDC-MM model with substrate (histidine) docked into the active site pocket. PLP shown as solvent accessible surface and protein residues as sticks. Histidine marked with 'SUB' is presented as ball & sticks.

In substrate binding, the side chain of l-histidine is surrounded by residues: Glu-29, Ser-30, His-231 and Lys-232 (*figure 5*). The oxygen atoms of Glu-29 and Ser-30 positioned above the imidazole ring of the substrate. N<sub>2</sub> of l-histidine (substrate) forms a hydrogen bond with main-chain oxygen atom of Ser-30. The carboxylate group of substrate forms a salt bridge with N<sub>Z</sub> of Lys-232. The imidazole ring of the substrate and His-231 are oriented towards the same plane. The side chain nitrogen atom of Lys-232 (N<sub>Z</sub>) forms salt bridge network with the  $\alpha$ -carboxylate group of l-histidine (substrate) and oxygen atoms (O<sub>1</sub> and O<sub>2</sub>) from Glu-29 structure.

*Figure 6* represents 2-amino-2-methyl 3(benzimidazole) propionic acid (BMP) which fits into the substrate binding site by forming several interactions with the HDC-MM active site residues such as; Glu-29, Ser-30, His-231 and Lys-232.

The benzimidazole ring of BMP is located in the position which is occupied by the substrate, histidine, and its ring is directed toward the imidazole ring of His-231 while forming hydrogen bonds between the nitrogen atom of BMP and N<sub>2</sub> of His-231. At the same time, BMP could interact with the oxygen atom (O<sub>1</sub>) of Glu-29 and

the main-chain oxygen atoms of Lys-232 and Ser-30 through hydrogen bonds.

In conclusion, the present homology modelling and docking suggest that the HDC-MM has a fold generally compatible with that of the AAT-EC. Despite some limitations of the methods used, the homology model of HDC-MM presented here provides a useful approach for further experiments and agree fairly well with the biochemical results [19].

## Acknowledgements

Most of this study was carried out in EMBL and DKFZ, Heidelberg, Germany. Financial support for this work was provided by a grant to F.S.T. and B.H. from the Iran Ministry of Health and Medical Education and in part by the research fellowship from EMBL and DKFZ. The authors especially acknowledge Prof. Dr Hartmut Oschkinat for his generosity in allowing us to use computing facilities in EMBL. We are most grateful to our colleague Dr A.M. Sobhani for his kind help in preparing colour figures. We would also like to thank F.J. Nouri for his kind assistance.



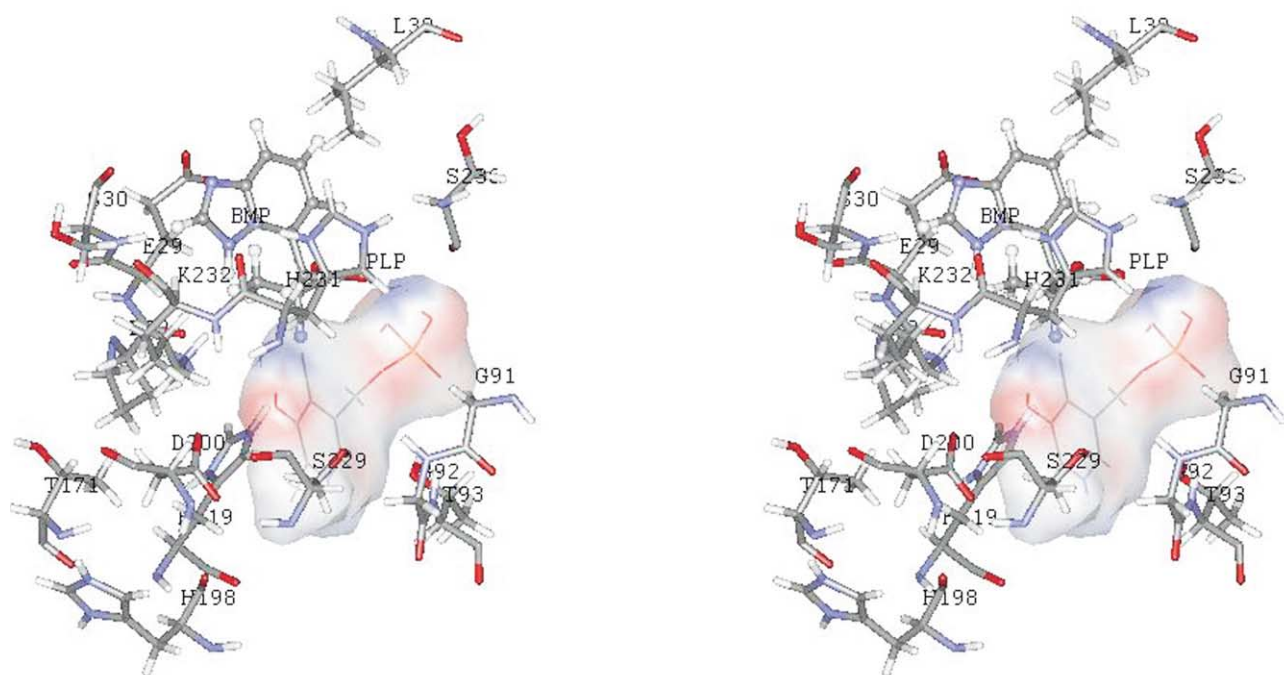


**Figure 6.** The proposed compound as a potential inhibitor of l-histidine decarboxylase 2-amino-2-methyl-3(2-benzimidazole) propionic acid (BMP), docked into the active site of the target protein (HDC-MM model). PLP shown as solvent accessible surface and protein residues as sticks. Ball & sticks represent BMP.

## References

- [1] Yatsunami K., Fukui T., Yakugaku. Zasshi 114 (1994) 803–822.
- [2] Snell E.E., Ann. NY Acad. Sci. 585 (1990) 1–12.
- [3] Ohmori E., Fukui T., Imanishi N., Yatsunami K., Ichikawa A., J. Biochem. 107 (1990) 834–839.
- [4] Kamath A.V., Vaaler G.L., Snell E.E., J. Biol. Chem. 266 (1991) 9432–9437.
- [5] Beaven M.A., Monographs in Allergy, Basel, 1978, p. 13.
- [6] Kahlson G., Rosengren E., Svahn D., Thunberg R., J. Physiol. Lond. 174 (1964) 400–416.
- [7] Douglas W.W., The Pharmacological Basis of Therapeutics, 1975, pp. 589–629.
- [8] Schwartz J.C., Garberg M., Pollard H., Handbook of Physiology 4, 1986, pp. 257–358.
- [9] Hough L.B., Prog. Neurobiol. 30 (1988) 469–505.
- [10] Acuna Y., Mathison Y., Campos H.A., Israel A., Inflamm. Res. 47 (1998) 109–114.
- [11] Bartholyns J., Bouclier M., Cancer Res. 44 (1984) 639–645.
- [12] Suonio E., Tuomisto L., Alhava E., Agents Actions 41 (1994) 118–120.
- [13] Circeo G., Engel N., Croci M., Davio C., Martin G., Fitzimons C., Bergoc R., Rivera E., Inflamm. Res. 46 (1997) 59–60.
- [14] Watanabe T., Yamatodani A., Maeyama K., Wada H., Trends Pharmacol. Sci. 11 (1990) 363–367.
- [15] Aures D., Hakanson R., Clark W., Handbook of Neurochemistry Vol. IV, Plenum, NY, 1970, pp. 165–198.
- [16] Aures D., Hakanson R., Methods Enzymol. 17 (1971) 667–677.
- [17] Schayer R.W., Handbook of Experimental Pharmacology 18/2, 1971, pp. 109–129.
- [18] Tanase S., Guirard B.M., Snell E.E., J. Biol. Chem. 260 (1985) 6738–6746.
- [19] Vaaler G.L., Snell E.E., Biochemistry 28 (1989) 7306–7313.
- [20] Shakila R.J., Vasundhara T.S., Rao D.V., Z. Lebensm. Unters. Forsch. 203 (1996) 71–76.
- [21] Hayashi H., Tanase S., Snell E.E., J. Biol. Chem. 261 (1986) 11003–11009.
- [22] Guirard B.M., Snell E.E., J. Bacteriol. 169 (1987) 3963–3968.
- [23] Tran V.T., Snyder S.H., J. Biol. Chem. 256 (1981) 680–686.
- [24] Taguchi Y., Watanabe T., Kubota H., Hayashi H., Wada H., J. Biol. Chem. 259 (1984) 5214–5221.
- [25] Feldberg R.S., Iannitt D.A., Cochrane D.E., Biochem. J. 249 (1988) 197–300.
- [26] Suzuki S., Tanaka S., Nemoto K., Ichikawa A., FEBS Lett. 437 (1998) 44–48.
- [27] Riley W.D., Snell E.E., Biochemistry 7 (1968) 3520–3528.

- [28] Recsei P.A., Snell E.E., *J. Biol. Chem.* 257 (1982) 7196–7202.
- [29] Gallagher T., Snell E.E., Hackert M.L., *J. Biol. Chem.* 264 (1989) 12737–12743.
- [30] Van Poelje P.D., Snell E.E., *Ann. Rev. Biochem.* 59 (1990) 29–59.
- [31] Gallagher T., Rozwarzki D.A., Ernst S.R., Hackert M.L., *J. Mol. Biol.* 230 (1993) 516–528.
- [32] Singh S., Johnson P.I., Javed A., Gray T.S., Lonchyna V.A., Wurster R.D., *Circulation* 99 (1999) 411–419.
- [33] Christen P., Metzler D.E., *Transaminases*, J. Wiley and Sons, NY, 1985.
- [34] Christenson J.G., Dairman W., Udenfriend S., *Arch. Biochem. Biophys.* 141 (1970) 356–367.
- [35] Markovic-Housley Z., Kania M., Vincent M.G., Jansonius J.N., John R.A., *Biochemistry of Vitamin B6*, Basel, 1987, pp. 187–190.
- [36] Momany C., Ghosh R., Hackert M.L., *Protein Science* 4 (1995) 849–854.
- [37] Toney M.D., Hohenester E., Keller J.W., Jansonius J.N., *J. Mol. Biol.* 245 (1995) 151–179.
- [38] Momany C., Ernst S., Ghosh R., Chang N.L., Hackert M.L., *J. Mol. Biol.* 252 (1995) 643–655.
- [39] Engel N., Olmo M.T., Coleman C.S., Medina M.A., Pegg A.E., Sanchez-Jimenez F., *Biochem. J.* 320 (1996) 365–368.
- [40] Osterman A.L., Brooks H.B., Rizo J., Phillips M.A., *Biochemistry* 36 (1997) 4558–4567.
- [41] Rosso G., Takashima K., Adams E., *Biochem. Biophys. Res. Commun.* 34 (1969) 134–140.
- [42] Gani D., *Phil. Trans. R. Soc. Lond. B* 332 (1991) 131–139.
- [43] Alexander F.W., Sandmeier E., Mehta P.K., Christen P., *Eur. J. Biochem.* 219 (1994) 953–960.
- [44] Smith D.L., Almo S.C., Toney M.D., Ringe D., *Biochemistry* 28 (1989) 8161–8167.
- [45] Okamoto A., Higuchi T., Hirotsuk K., Karamitsu S., Kagamiyama H., *J. Biochem.* 116 (1994) 95–107.
- [46] Malashkevich V.N., Strokopytov B.V., Borisov V.V., Dauter Z., Wilson K.S., Torchinsky Y.M., *J. Mol. Biol.* 247 (1995) 111–124.
- [47] Mollova E.T., Metzler D.E., Kintanar A., Kagamiyama H., Hayashi H., *Biochemistry* 36 (1997) 4558–4567.
- [48] Boecker E.A., Snell E.E., *Enzymes* 6, Academic Press, NY, 1972, pp. 217–253.
- [49] Hayashi H., Wada H., Yoshimura T., Esaki N., Soda K., *Ann. Rev. Biochem.* 59 (1990) 87–110.
- [50] Higgins D.G., Bleasby, Funchs, ClustalW multiple alignment program. *CABIS* 8 (1991) 189–191.
- [51] Rost B., Sander C., *J. Mol. Biol.* 232 (1993) 584–599.
- [52] Biosym., *Manual for Insight II*. San Diego, California: Biosym Technologies, Inc., (1993).
- [53] Divella S., MOPAC: A general molecular orbital package. *QCPE BULL.* 4 (1984) 109.
- [54] Stewart J.P., *QCPE Bull.* 3 (1983) 43.
- [55] Dewar M.J.S., Bisch E.G., Stewart J.P., *J. Am. Chem. Soc.* 107 (1985) 3902–3909.
- [56] Hofer J.M., *Conformations in Biology and Drug Design* 7, 1985, pp. 213–299.
- [57] Vriend G., *J. Mol. Graph.* 8 (1990) 52–56.
- [58] Laskowski R.A., Macarthur M.W., Moss D.S., Thornton J.M., *J. Appl. Crystallog.* 26 (1993) 283–291.
- [59] Sandmeier E., Hale T.I., Christen P., *Eur. J. Biochem.* 221 (1994) 997–1002.
- [60] Bashford D., Chotia C., Lesk A.M., *J. Mol. Biol.* 196 (1987) 199.
- [61] Smith D.M., Gani T.D., *Experientia* 47 (1991) 1104–1118.
- [62] Yano T., Yasunari H., Chen V.J., Metzler D.E., Miyahara I., Hirotsu K., Kagamiyama H., *J. Mol. Biol.* 234 (1993) 1218–1229.
- [63] Kirsch J.F., Eichele G., Ford G.C., Vincent M.G., Jansonius J.N., *J. Mol. Biol.* 174 (1984) 497–525.
- [64] Engel N., Olmo M.T., Coleman C.S., Medina M.A., Pegg A.F., Sanchez-Jimenez F., *Biochem. J.* 320 (1996) 365–368.
- [65] Sakamoto Y., Watanabe T., Hayashi H., Taguchi Y., Wada H., *Agents Actions* 17 (1985) 32–37.